Modelling the structure of the red cell membraneThis paper is one of a selection of papers published in a Special Issue entitled CSBMCB 53rd Annual Meeting Membrane Proteins in Hea...

Article *in* Biochemistry and Cell Biology · March 2011

DOI: 10.1139/o10-154 · Source: PubMed

CITATIONS
102

READS
992

2 authors, including:

Lesley Jean Bruce
N.H.S. Blood and Transplant, Filton, Bristol, UK
85 PUBLICATIONS **3,751** CITATIONS

REVIEW / SYNTHÈSE

Modelling the structure of the red cell membrane[1]

Nicholas M. Burton and Lesley J. Bruce

Abstract: The red cell membrane has long been the focus of extensive study. The macromolecules embedded within the membrane carry the blood group antigens and perform many functions including the vital task of gas exchange. Links between the intramembrane macromolecules and the underlying cytoskeleton stabilize the biconcave morphology of the red cell and allow deformation during microvascular transit. Much is now known about the proteins of the red cell membrane and how they are organised. In many cases we have an understanding of which proteins are expressed, the number of each protein per cell, their oligomeric state(s), and how they are collected in large multi-protein complexes. However, our typical view of these structures is as cartoon shapes in schematic figures. In this study we have combined knowledge of the red cell membrane with a wealth of protein structure data from crystallography, NMR, and homology modelling to generate the first, tentative models of the complexes which link the membrane to the cytoskeleton. Measurement of the size of these complexes and comparison with known cytoskeletal distance parameters suggests the idea of interaction between the membrane complexes, which may have profound implications for understanding red cell function and deformation.

Key words: erythrocyte, band 3 macrocomplex, protein 4.1 junctional complex, lipid bilayer, protein modelling.

Résumé : La membrane des érythrocytes a fait l'objet de recherches intensives depuis longtemps. Les macromolécules implantées dans la membrane portent les antigènes des groupes sanguins et exercent plusieurs fonctions, notamment la tâche vitale d'assure les échanges gazeux. Les liens entre les macromolécules intra-membranaires et le cytosquelette sous-jacent stabilisent la morphologie biconcave des érythrocytes et permettent leur déformation lors du transit microvasculaire. On connaît assez bien les protéines de la membrane des érythrocytes et la façon dont elles sont organisées. Dans plusieurs cas, nous comprenons comment ces protéines sont exprimées, le nombre de chacune des protéines par cellule, leur(s) état(s) oligomérique(s), et la façon dont elles se regroupent en larges complexes multiprotéiques. Cependant, nous voyons typiquement ces structures de façon schématique. Dans cette étude, nous avons combiné les informations relatives à la membrane des érythrocytes et un ensemble de données recueillies sur la structure des protéines par cristallographie, RMN et modélisation par homologie, afin de générer les premiers modèles provisoires des complexes qui lient la membrane au cytosquelette. La mesure de la taille de ces complexes et sa comparaison aux paramètres de distance du cytosquelette connus suggère l'idée d'une interaction entre les complexes membranaires, laquelle pourrait avoir des implications importantes dans la compréhension de la fonction et de la déformation des érythrocytes.

Mots-clés : érythrocytes, complexe macromoléculaire de la Bande 3, protéine 4.1 du complexe de jonction, bicouche lipidique, modélisation des protéines.

[Traduit par la Rédaction]

Introduction

The red cell membrane has been studied extensively for many years and much is known about its composition. Red cells provided a readily accessible source for early studies of basic membrane structure (e.g., Steck et al. 1970; Marchesi and Steers 1968; Schrier 1963; da Silva and Branton 1970). Interest in the specialized nature of the red cell membrane increased with the classification of the blood group antigens associated with the red cell (Race and Sanger 1975). Many of these antigens caused transfusion reactions and were therefore important for transfusion medicine (Klein and Anstee 2005). Slowly over the past 40 years the membrane proteins that carry these antigenic structures have been identified (Daniels 1995; Reid and Lomas-Francis 2004). These proteins vary enormously in their functions, from ion trans-

Received 3 August 2010. Revision received 13 October 2010. Accepted 15 October 2010. Published on the NRC Research Press Web site at bcb.nrc.ca on 16 March 2011.

N.M. Burton. School of Biochemistry, University of Bristol, BS8 1TD, UK; Bristol Institute for Transfusion Sciences, N.H.S. Blood and Transplant, North Bristol Park, Filton, Bristol, BS34 7QH, UK.
L.J. Bruce.[2] Bristol Institute for Transfusion Sciences, N.H.S. Blood and Transplant, North Bristol Park, Filton, Bristol, BS34 7QH, UK.

[1]This paper is one of a selection of papers published in a Special Issue entitled CSBMCB 53rd Annual Meeting — Membrane Proteins in Health and Disease, and has undergone the Journal's usual peer review process.
[2]Corresponding author (e-mail: lesley.bruce@nhsbt.nhs.uk).

porters such as band 3 (AE1, *SLC4A1*), which carries the Diego antigens, or adhesion proteins such as the Lutheran glycoprotein (Lu, *LU*), to complement inhibitors such as Daf (CD55, *CD55*), which carries the Cromer antigens. We have listed some of the proteins of the red cell membrane in Table 1. Many of these proteins are multi-spanning membrane proteins, which are notoriously difficult to crystallize, so there has been very little idea of the structure of these proteins. Until now structural predictions have depended on biochemical analysis: hydropathy plots to define the membrane-spanning domains; antigenic sites and glycan-binding sites to define extracellular domains; and proteolytic sites, antibody binding, and chemical modification to define intracellular domains. It has only been in very recent years that crystal structures for some red cell membrane proteins, or for their homologues, have become available.

The red cell has a distinctive biconcave (or doughnut) shape and is highly deformable (Li et al. 2007). The forces that maintain this shape and flexibility are of great interest because defects in these forces can result in haemolytic anaemia. Early electron microscopy of freeze-fractured red cells showed a highly structured hexagonal cytoskeleton (when extended) and a membrane containing intramembranous particles of about 8–12 nm in size evenly distributed over the cell (Liu et al. 1987). These particles were thought to comprise protein complexes.

The study of misshapen red cells (spherocytes, elliptocytes, ovalocytes) has informed our understanding of the interactions between proteins of the red cell membrane (An and Mohandas 2008; Gallagher 2004). It became clear that disruptions to the horizontal interactions of the spectrin skeleton resulted in elliptocytes, whereas disruption of the vertical interactions, linking the membrane to the cytoskeleton, resulted in spherocytes (Lux and Palek 1995). Formation of ovalocytes, stomatocytes, and echinocytes seemed to involve a change in the hydration of the red cell (Bruce 2008; Rinehart et al. 2010). In recent years more data have come to light about the proteins that form the major complexes and the links that they form with the cytoskeleton. We have put these data together with the current knowledge of the protein structures to estimate the size of many of the major red cell membrane proteins, allowing us to build a more realistic model of how the membrane may look. The membrane obviously contains many other proteins that may be freely mobile or have yet to be assigned to a complex, and "new" red cell proteins are being discovered regularly in the many recent proteomic studies (reviewed in Liumbruno et al. 2010). However, these more minor components of the red cell membrane are beyond the scope of this review. We will concentrate on the major complexes to create a model of the membrane based on X-ray crystal structures, NMR structures, and homology models of red cell membrane proteins, and we will discuss the implications of this model.

Structure of the red cell membrane

Red cell cytoskeleton

Underlying the red cell membrane is a hexagonal lattice of spectrin. Spectrin consists of antiparallel heterodimers of α-spectrin and β-spectrin. The heterodimers associate head to head to form tetramers and it is these tetramers that form the cross-links of the hexagonal lattice. Spectrin tetramers are ~200 nm in length when extended but can contract to just 70 nm (Kodippili et al. 2010). The junctions of the cytoskeleton lattice are formed by filaments of β-actin, protein 4.1, and associated proteins (Fig. 1). Periodically along the cytoskeletal lattice there are proteins that link the cytoskeleton to the membrane. Ankyrin binds to β-spectrin, about one third of the distance along the spectrin tetramer, forming an important vertical link between the cytoskeleton and the membrane proteins (Stabach et al. 2009; La-Borde et al. 2010). The association of ankyrin with band 3 is the most critical vertical interaction. When this is disrupted either through loss of ankyrin, loss of band 3, or mutations in the ankyrin–band 3 binding site, the red cells become spherocytic and extremely unstable (Delaunay 2007). Ankyrin can also bind other membrane proteins. The Rh-associated glycoprotein (RhAG) is thought to bind ankyrin (Nicolas et al. 2003), but this interaction cannot be as important as that between band 3 and ankyrin, as loss of RhAG in Rh_{null} cells simply results in stomatocytosis (Anstee and Tanner 1988). Other proteins such as CD44 and the NaK-ATPase bind ankyrin, but these are relatively minor components (6×10^3 to 10×10^3 and 0.5×10^3 copies per red cell, respectively) and cannot have the same impact as the band 3–ankyrin association (with 1.2×10^6 and 1.2×10^5 copies per red cell, respectively). In fact ankyrin may bind certain proteins to bring them together to form the band 3 macrocomplex, which is described below. At the cytoskeletal junctions, protein 4.1 not only stabilizes the β-actin–spectrin association but also binds the membrane protein glycophorin C (GPC) and the associated peripheral protein p55 (Hemming et al. 1995), forming another important vertical link. Other interactions between the membrane and the actin junctions have been reported recently and will be described below.

Band 3 macrocomplex

The composition of the band 3 macrocomplex was originally proposed based on the proteins that were absent in band 3_{null} red cells (Ribeiro et al. 2000; Bruce et al. 2003). Proteins known to associate with band 3, such as ankyrin, protein 4.2, and glycophorin A (GPA), were absent or reduced in these cells, as expected, but the proteins of the Rh complex (RhAG, RhCE, RhD, CD47, LW, glycophorin B (GPB)) were also absent or reduced, showing that these proteins associate with band 3 in normal red cells (Bruce et al. 2003). The copy number of RhAG is uncertain (100 000 – 200 000, Gardner et al. 1991), as is the oligomeric state. Until recently the core of the Rh complex was thought to comprise two RhAG and two Rh polypeptides, forming a tetramer (Eyers et al. 1994). However, other members of the ammonia transport family form trimers, and a close homologue of RhAG has recently been crystallized and found to form a trimer (Gruswitz et al. 2010); it is therefore very likely that the core of the Rh complex is a trimer, probably composed of one RhAG and two Rh polypeptides, although RhAG can also be expressed alone (but at much reduced levels) without the Rh polypeptides (Rh_{null} amorph type, Kato-Yamazaki et al. 2000). The stoichiometry of Rh complexes, about 100 000 copies per red cell, and the evidence that there is an interaction between RhAG and ankyrin (Nicolas et al. 2003) suggest that these proteins associate with

Table 1. Some proteins of the red cell membrane.

Protein name	Antigen name	Gene	M_r (gel) ($\times 10^3$)*	No. of amino acids	No. of copies ($\times 10^3$)	Oligomeric state	Chromosome location	Reference for copy number
α-Spectrin		*SPTA1*	240	2429	242	Heterodimer (tetramer)	**1**q22–q23	Lux and Palek 1995
β-Spectrin		*SPTB*	220	2137	242	Heterodimer (tetramer)	**14**q23–q24	Lux and Palek 1995
Ankyrin		*ANK1*	210	1880	124	Monomer	**8**p11.2	Lux and Palek 1995
α-Adducin		*ADD1*	103	737	30	Heterodimer	**4**p16.3	Lux and Palek 1995
β-Adducin		*ADD2*	97	726	30	Heterodimer	**2**p13.3	Lux and Palek 1995
AE1 (band 3)	Diego	*SLC4A1*	90–100	911	1200	Dimer or tetramer	**17**q21–q22	Steck 1978; Jay and Cantley 1986
Protein 4.1		*EPB41*	80/78	588	200	Monomer	**1**p36.2–p34	Goodman et al. 1982
Protein 4.2		*EPB42*	72	691	250	Dimer or trimer?	**15**q15	Lux and Palek 1995
Dematin (band 4.9)		*EPB49*	48/52	383	140	Trimer	**8**p21.1	Lux and Palek 1995
p55		*MPP1*	55	466	80	Dimer	**X**q28	Lux and Palek 1995
β-Actin		*ACTB*	43	375	500	Oligomer (∼14)	**7**p15–p12	Lux and Palek 1995
Tropomodulin		*TMOD1*	43	359	30	Monomer	**9**q22	Lux and Palek 1995
G3PD		*GAPD*	35	335	500	Tetramer	**12**p13	Lux and Palek 1995
Stomatin (band 7)		*STOM*	31	288	10	—	**9**q34	
Tropomyosin		*TPM3*	27/29	239	70	Heterodimer	**1**q21	Lux and Palek 1995
Peroxiredoxin-2		*PRDX2*	23	198	200	Dimer (decamer)	**19**p13.2	Lux and Palek 1995
Glycophorin A	MNS	*GYPA*	36	131	1000	Dimer	**4**q31	Gardner et al. 1989
Glycophorin B	MNS	*GYPB*	20	72	250	Dimer	**4**q31	Gardner et al. 1989
Glycophorin C	Gerbich	*GYPC*	32	128	135	Dimer?	**2**q14–q21	Smythe et al. 1994
Glycophorin D	Gerbich	*GYPC*	23	107	50	Dimer?	**2**q14–q21	Smythe et al. 1994
Glycophorin E		*GYPE*	—	59	—	—	**4**q31	
AChE	Yt	*ACHE*	72, 160	617	10		**7**q22	Reid and Lomas-Francis 2004
Aquaporin 1	Colton	*AQP1*	28 (40–60)	269	120–160	Tetramer	**7**p14.3	Preston et al. 1994
CAII		*CA2*	29	260	100		**8**q22	Sterling et al. 2001
CAIV		*CA4*	36, 55	312			**17**q23	
CD44	Indian	*CD44*	80	742	6–10		**11**p13	Anstee et al. 1991
CD47		*CD47*	47–52	323	10–50	Monomer	**3**q13.2	Gardner et al. 1991
CD58 (LFA-3)		*CD58*	55–70	250	3–7		**1**p13	Anstee et al. 1991
CD59 (complement regulation)		*CD59*	18–20	128	20–40		**11**p13	Fletcher et al. 1992
CD99		*CD99*	32.5	163	1		**X**p22.32	Reid and Lomas-Francis 2004
CR1	Knops	*CR1*	190, 220	2039	0.02–1.5		**1**q32	Reid and Lomas-Francis 2004
DAF (CD55)	Cromer	*CD55*	60–70	381	20		**1**q32	Reid and Lomas-Francis 2004
ADP-ribosyltransferase	Dombrock	*ART4*	47–58	314			**12**p13–p12	
Duffy		*FY*	35–45	338	6–13		**1**q23.2	Riwom et al. 1994
Flotillin 1		*FLOT1*	48	427			**6**p21.3	
Flotillin 2		*FLOT2*	42	379			**17**q11–q12	
Glut1		*SLC2A1*	45–65	492	200–700		**1**p34.2	Reid and Lomas-Francis 2004
Kell glycoprotein	Kell	*KEL*	93	732	3–18		**7**q33	Parsons et al. 1993

Table 1 (*concluded*).

Protein name	Antigen name	Gene	M_r (gel) ($\times 10^3$)*	No. of amino acids	No. of copies ($\times 10^3$)	Oligomeric state	Chromosome location	Reference for copy number
KX	Kx	*XK*	37	444			**X**p21.1	
Lutheran glycoprotein	Lu	*LU*	78/85	597	1.5–4		**19**q13.2	Merry et al. 1987
LW glycoprotein	LW	*ICAM4*	37–43	241	3–5		**19**p13.2	DeVeber et al. 1971
MCT1 (lactate transport)		*SLC16A1*	54				**1**p12–13	
NaK-ATPase		*ATP1A2*		1020	0.5		**1**q21–23	
Nucleoside transporter		*SLC29A1*	55	456	10		**6**p21.1–p21.2	Reid and Lomas-Francis 2004
RhAG		*RHAG*	45–100	409	100–200	Heterotetramer	**6**p21.1–p11	Gardner et al. 1991
Rh polypeptide	Rh	*RHCE*, *RHD*	30/32	~410	200 (D and CE)	Heterotetramer	**1**p36.11	Gardner et al. 1991
ERMAP	Scianna	*ERMAP*	60–68	475			**1**p34.2	
Urea transporter	Kidd, Jk	*SLC14A1*	43	389	14		**18**q11–q12	Mannuzzu et al. 1993
XG glycoprotein	Xg	*XG*	22–29	180	9		**Xp**22.32	Reid and Lomas-Francis 2004

*M_r: apparent molecular weight in a Laemmli gel buffer system.

Fig. 1. Band 3 complexes in the red cell membrane form a lattice of interacting protein complexes above a cytoskeletal lattice of proteins. Spacing of the band 3 complexes is probably organised by the cytoskeleton. Band 3 associates with glut1, which associates with stomatin, so some "free" dimeric complexes may reside in lipid rafts.

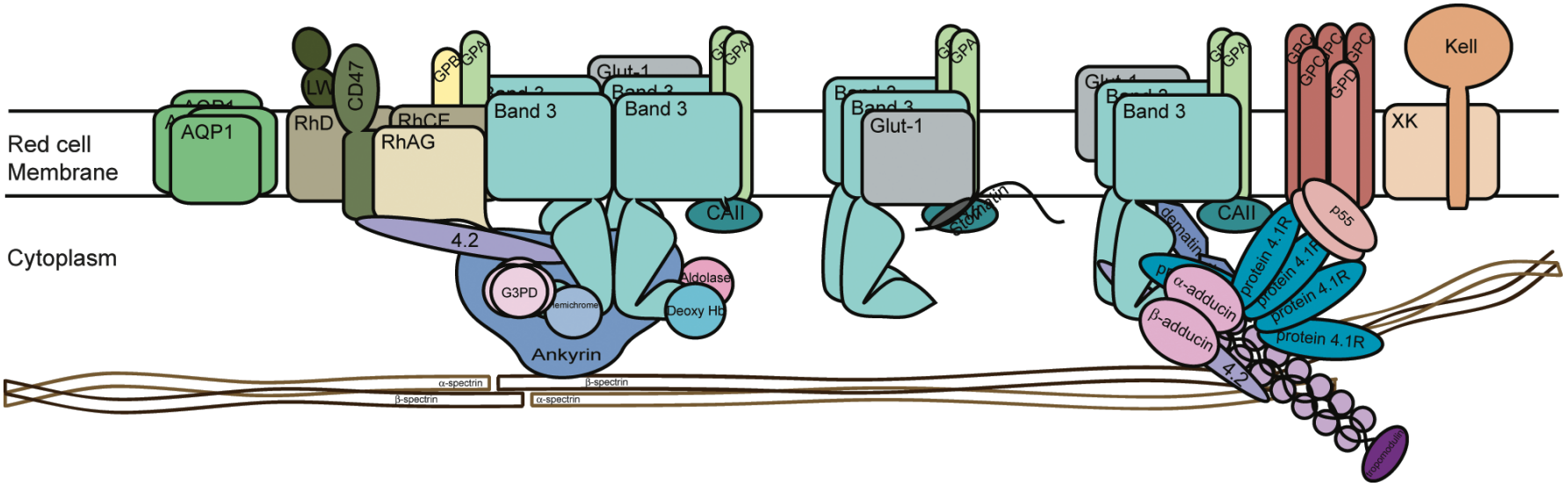

the tetrameric form of band 3, which associates with ankyrin and is present at about 120 000 copies per red cell.

Stoichiometry and copy number inform our understanding of complex composition. Band 3 is present at about 1.2×10^6 copies per red cell and is often quoted as being present in the red cell membrane as dimers (60%, 360 000 copies) and tetramers (40%, 120 000 copies). This ratio is based partly on the size-exclusion HPLC analysis of band 3 extracted by $C_{12}E_8$, which was used to determine the amount of band 3 associated with ankyrin (42%, 58%) (Liu et al. 1995). It is also based on the fact that band 3 is dimeric in the absence of ankyrin (Casey and Reithmeier 1991) and the presence of ankyrin induces the formation of band 3 tetramers (Michaely and Bennett 1995; Thevenin and Low 1990). Ankyrin is present at about 120 000 copies per red cell and binds to β-spectrin. Both α-spectrin and β-spectrin are present at about 240 000 copies per cell. The spectrins form heterotetramers, of which there are about 120 000 copies per cell. Together these data suggest that there are about 120 000 band 3 tetramers per red cell.

However, how these tetramers form is not fully understood. In studies of binding of ankyrin to inside-out membrane vesicles, band 3–ankyrin binding was found to have fast and slow kinetics; fast binding was thought to correspond to the binding of ankyrin to preexisting tetramers whereas slow binding corresponds to the binding of two dimers (Thevenin and Low 1990). What stabilizes these preformed tetramers is not known. It may be that other components of the band 3 macrocomplex, perhaps GPA–GPB heterodimers and RhAG–RhCE, cross-link the band 3 dimers into a stable conformation (Fig. 1). GPB is present at about 200 000 copies per red cell, whereas there are about 1×10^6 copies of GPA. Together they could form sufficient dimers to associate with every band 3 dimer. GPB is known to associate with RhAG, acting as a chaperone to RhAG in much the same way as GPA chaperones band 3 (Ridgwell et al. 1994; Groves and Tanner 1992). Perhaps band 3 dimers associate with GPA dimers and band 3 dimers that will form tetramers associate with GPA–GPB heterodimers. It would be interesting to measure the kinetics of ankyrin binding in the absence of the Rh complex to see whether ankyrin binding still showed fast kinetics.

Early electron microscopy of freeze-fractured red cells showed that normal cells contain about 5373 intramembranous particles (IMPs) per μm^2 (Yawata 2003). Red cells that lack band 3 contain 70% fewer IMPs, only about 1856 per μm^2 (Yawata 2003). This suggests that about 3517 IMPs per μm^2 are band 3 complexes. The surface area of a red cell is about 136 μm^2, so there would be about 478 312 IMPs per red cell containing band 3. This correlates well with there being 120 000 band 3 tetramers and 360 000 band 3 dimers. However, electron microscopy studies using the surface replica method and anti-GPA+GPB antibodies showed only 600 particles per μm^2 for GPA+GPB compared with 3517 per μm^2 for band 3 (Yawata 2003). It is possible that the application of the antibodies induced clustering in this study, but it is also possible that these results reflect the in vivo state. This introduces the intriguing possibility that the glycophorins do not associate stoichiometrically, i.e., one GPA–GPA or GPA–GPB dimer associating with one band 3 dimer, but that they may cluster and associate with only one form of band 3 complex. GPA exists only as a dimer, so the 600 particles must contain at least 1 200 GPA (or GPB) molecules. This poses the possibility that five GPA–GPA (or GPA–GPB) dimers cluster with the band 3 macrocomplex, or that GPA–GPA (or GPA–GPB) dimers cluster independently in the membrane, only brought together with band 3 by the application of anti-GPA antibodies (the Wr^b epitope comprises Glu658 of band 3 and residues 58–70 of GPA) (Bruce et al. 1995). Interestingly, there is evidence that glycophorins C and D cluster in the junctional complex (see below).

Actin junctional complex

The core actin junctional complex comprises 15–20 β-actin molecules in two filaments (8–10 molecules per filament) wrapped around a dimer of tropomyosin and capped by tropomodulin (Weber et al. 1994). The actin filament interacts directly with β-spectrin (An et al. 2005) and is stabilized by the cross-linking of protein 4.1, which binds both β-spectrin and actin (Becker et al. 1990). The junctional complex includes other actin-binding proteins including dematin and the actin-bundling proteins α- and β-adducin, thought to limit the size of the actin filaments to about 35 nm (Mische et al. 1987). The junctional complex is known to interact with the membrane proteins glycophorin C (GPC) and glycophorin D (GPD) via the scaffolding protein p55 and protein 4.1 (Hemming et al. 1995). Loss of GPC in GPC_{null} individuals or loss of protein 4.1 results in elliptocytic red cells (Anstee et al. 1984; Daniels et al. 1986; Delaunay 2007).

The number of junctional complexes per red cell is probably about 40 000. This number is partly based on the amount of spectrin and ankyrin in the red cell. The cytoskeleton forms a hexagonal lattice which can be broken down into repeating "cytoskeleton elements" (Fig. 2), each element containing one junctional complex, three spectrin tetramers, three ankyrins, three band 3 tetramers, one band 3 dimer associated with the junctional complex, and approximately four free band 3 dimers (Fig. 2*a*). If each cytoskeleton element has three spectrin tetramers and three ankyrins and there are 120 000 of each, then there must be ~40 000 junctions per cell. This estimate fits well with the estimated copy number per cell for the other junctional components: actin, about 500 000 (15–20 per junction, Weber et al. 1994); tropomyosin, about 35 000 dimers per cell; tropomodulin, about 30 000 monomers; dematin, about 45 000 trimers; and α-adducin and β-adducin, about 30 000 heterodimers (Lux and Palek 1995). There are reportedly 200 000 copies of GPC and GPD together (Smythe et al. 1994). However, this number was measured using Fab fragments of GPC antibodies, and the intact antibodies gave very different results (7 000, 29 500, and 48 000 molecules per red cell for BRAC1 (IgM), BRAC 11 (IgG), and BRIC10 (IgG)). It was suggested that this discrepancy was due to clustering of the GPC and GPD proteins at the junctions and that the Fab fragments measured the actual numbers of molecules whereas the intact antibodies measured the number of clusters (Smythe et al. 1994). Thus, there are probably about five molecules of GPC and/or GPD at each junction, perhaps one GPD and four GPC (Fig. 1). Similarly, there are about 200 000 copies of protein 4.1 per red cell

Fig. 2. The structure of the cytoskeleton. (*a*) The cytoskeleton forms a hexagonal lattice. (*b*) This can be depicted as repeat elements, with one cytoskeleton element containing one junctional complex, three spectrin tetramers, three ankyrins, three band 3 tetramers, one band 3 dimer associated with the junctional complex, and approximately four free band 3 dimers (not shown). (*c*) As discussed in this review, the size of the junctional complex is ~20 nm by 17 nm, the macrocomplex is ~17.5 nm by 14 nm, and an band 3 dimer is ~9 nm by 4 nm. When these complexes are drawn (diagrammatically to scale) on a contracted spectrin skeleton it can be seen that the proteins of the different complexes could come in close contact.

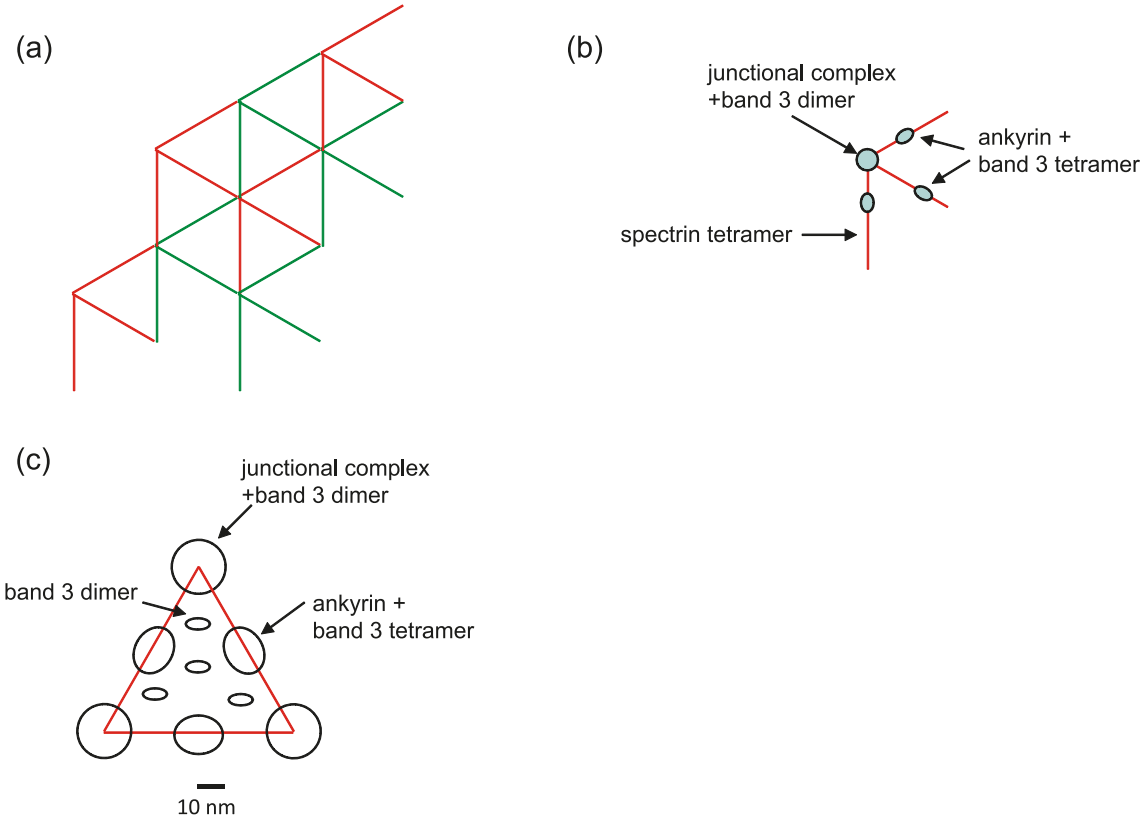

(Goodman et al. 1982), providing about five protein 4.1 molecules per junction (Fig. 1).

Recent studies have described other links between the membrane and the junctional complex. One study suggests that the erythrocyte glucose transporter, glut1, associates with dematin, forming a novel link (Khan et al. 2008). Another study shows that α- and β-adducin interact with dimeric band 3, forming another link (Anong et al. 2009). Yet another study shows that protein 4.2 interacts with the carboxyl-terminal EF-hands of α-spectrin, which is located in the junctions (Korsgren et al. 2010). Using immunoprecipitation studies, we have shown that glut1 associates with band 3 (L.J. Bruce, unpublished data, July 2010). All the above point to the inclusion of at least one band 3 dimer in the junctional complex. Studies of protein 4.1 knockout mice have suggested that in the mouse red cell membrane the junctional complex includes even more proteins (An and Mohandas 2008). The chemokine receptor (Duffy), Kell, Kx, and the Rh protein were all found to be reduced in protein 4.1 deficient mouse red cells, suggesting that these proteins interact in the mouse red cell membrane (Salomao et al. 2008). We have studied the red cell membranes from a protein 4.1 deficient human and found similar results, except that the Rh protein was not altered in human protein 4.1_{null} red cells (L.J. Bruce, unpublished data, July 2010). Therefore it is quite likely that the junctional complex in human red cells includes Kell and Kx (Fig. 1). However, it must be remembered that these are minor components of the red cell and present only at about 5×10^3 to 15×10^3 copies (Table 1), so they cannot be included in every junction. Inclusion of the Duffy protein could not be established because the protein 4.1_{null} red cells studied were an unusual Duffy phenotype (L.J. Bruce, unpublished data, July 2010).

Band 3 dimers and lipid rafts

The remaining 640 000 band 3 molecules (1 200 000 minus 480 000 in tetramers and 80 000 in junction-associated dimers), or 320 000 band 3 dimers, are thought to move relatively freely in the membrane, although they are confined to the corrals formed by the underlying cytoskeletal mesh (Steck 1978). Given that there are about 40 000 junctions per red cell forming 40 000 cytoskeleton elements (Fig. 2*a*), each corral probably contains about four band 3 dimers (Fig. 2*b*). This dimeric band 3 may well be associated with GPA dimers and glut1; there are sufficient copies of these proteins to associate with all band 3 oligomers (Table 1). Glut1 is known to associate with stomatin, which leads to the speculation that some of these band 3 dimers may reside in lipid rafts, which may organise their distribution in the membrane. Either way, the evidence of the spacing of IMPs in the membrane suggests that all band 3 complexes are evenly distributed around the membrane, so even these

Table 2. Band 3 macrocomplex proteins.

Protein	Copy no. ($\times 10^3$)	Oligomeric state	Size (aa)	Domain		Structure	Structure shown in figure
				Description	aa		
Band 3	1200 (480? in macrocomplex)	Tetramer	911	Cytoplasmic domain	1–380	Crystal structure (PDB ID: 1hyn, Zhang et al. 2000)	Crystal structure. Orientation with respect to membrane domain is highly speculative.
				Membrane domain	380–911	Low-resolution crystal structure (Yamaguchi et al. 2010)	Crystal structure of bacterial ClC Cl/H exchanger (PDB ID: 1kpl, Dutzler et al. 2002). Low-resolution AE1 crystal structure shows that bacterial ClC Cl/H exchanger shares overall size and shape with AE1 membrane domain.
Protein 4.2	200	Monomer	691	Transglutaminase domain (pred.)	16–685	Homology model available (Satchwell et al. 2009)	Homology model. Expected to be of good quality, but the extended conformation shown is a speculative model of the postulated active conformation.
GPA	1000	Dimer	150	Extracellular domain	20–91	Largely disordered (pred.)	Not shown
				TM helix	92–114	NMR structure (PDB ID: 1afo, MacKenzie et al. 1997)	NMR structure
				Cytoplasmic domain	115–150	Largely disordered (pred.)	Not shown
GPB	250	Dimer	91	Extracellular domain	20–91	Largely disordered (pred.)	Not shown
				TM helix	60–81	Homology model possible	Homology model based on GPA NMR structure. Expected to be of reasonable quality.
				Cytoplasmic domain	82–91	Largely disordered (pred.)	Not shown
Glut1	200–700	Dimer	492	MFS transporter (pred.)	1–492	Homology model available (Salas-Burgos et al. 2004)	Homology model. Expected to be of good quality.
RhAG	100–200	Heterotrimer?	409	Gas transport?	1–409	Homology model available (Burton and Anstee 2008)	Homology model. Expected to be of good quality.
Rh	200	Heterotrimer?	417	Gas transport?	1–417	Homology model available (Burton and Anstee 2008)	Homology model. Expected to be of good quality.
CD47	10–50	Monomer	323	Immunoglobulin domain	12–136	Crystal structure available (PDB ID: 2jjt, Hatherley et al. 2008)	Crystal structure
				Membrane	142–290	Five TM helices (pred.)	Five-helix bundle taken from bacteriorhodopsin crystal structure (PDB ID: 2brd, Grigorieff et al. 1996). Packing may be very different, overall size expected to be similar.
LW	3–5	Monomer	271	Immunoglobulin domains	62–217	Homology model available (Spring et al. 2001)	Homology model. Expected to be of good quality.
				Membrane domain	241–261	TM helix (pred.)	Ab initio modelled ideal α-helix
				Cytoplasmic domain	262–271	Largely disordered (pred.)	Not shown
Ankyrin	120	Monomer	1881	N-terminal domain	1–45	Small helical bundle (pred.)	Not shown

Table 2 (*concluded*).

Protein	Copy no. ($\times 10^3$)	Oligomeric state	Size (aa)	Domain		Structure	Structure shown in figure
				Description	aa		
				23 ankyrin repeats	46–812	Crystal structure available for 12 repeats (PDB ID: 1n11, Michaely et al. 2002), SMR model available for remainder (SMR accession: P16157)	Model of entire region constructed from crystal structure and SMR model. Would be expected to be of reasonable quality.
					812–911	Largely disordered (pred.)	Not shown
				ZU5 domain	911–1068	Crystal structure available (PDB ID: 3f59, Ipsaro et al. 2009)	Crystal structure
					1069–1393	High degree of β-strands (pred.). Speculative model constructed with Phyre, based on titin crystal structure (PDB ID: 3b43, von Castelmur et al. 2008).	Homology model constructed with Phyre. Very speculative.
				Death domain	1394–1497	Crystal structure available (PDB ID: 2yvi, unpublished)	Crystal structure
				C-terminal domain	1498–1881	Some secondary structure (pred.)	Not shown

Note: PDB, Protein Data Bank; "pred.", predicted from sequence; TM, transmembrane; SMR, SWISS-MODEL Repository of homology models; Phyre, Protein Homology/analogY Recognition Engine (Kelley and Sternberg 2009).

"free" non-cytoskeleton-attached band 3 dimers must have restrictions on their ability to cluster (possibly due to charge repulsion of their carbohydrate chains).

A new model of the red cell membrane

With the continued growth of the protein structure databases we are at the stage where we can make reasonable predictions of the overall structural parameters for nearly all of the components of the red cell macrocomplexes. High-resolution structures are available for some fragments, e.g., band 3 cytoplasmic domain, GPA transmembrane helices. For other components, high-quality homology models may be constructed based on known structures with high degrees of sequence identity, e.g., ICAM-4 extracellular domain, Rh proteins. Other components require more speculative modelling to fill in the gaps. The molecular coordinates used in this study come from a variety of sources. Where possible we have used structures documented in previous published work. If such data are not available, we have searched the SWISS-MODEL Repository of homology models (Kiefer et al. 2009). For the remaining components we have performed sequence analysis and generated models with the Protein Homology/analogY Recognition Engine (Phyre) fold recognition server (Kelley and Sternberg 2009). Some of the models generated by this method are highly speculative, with very low sequence identity between target and template. While in some cases this will have resulted in incorrect prediction of the protein fold, the results will still be adequate for the assembly of crude models of the overall size of the multi-protein complexes. Phyre also identifies regions of protein sequence which are likely to be natively disordered; no attempt has been made to model these regions. It should be noted that while it is very challenging to characterize the structure of disordered regions, they are increasingly considered to be functionally important (Uversky and Dunker 2010). The components of the complexes and how they have been modelled are detailed in Tables 2 and 3.

Our models of the band 3 macrocomplex and the protein 4.1 junctional complex are shown in Figs. 3 and 4, respectively. It must be noted that the arrangement of proteins within the complexes is not based on experimental evidence and the intermolecular interactions have not been rigorously modelled. The complexes have been assembled in such a way as to pack the proteins as tightly as possible and satisfy certain known interactions. In our models there appears to be relatively little macromolecular mass on the extracellular side of the complexes. This is somewhat misleading, as substantial extracellular domains are predicted to be disordered and hence are not shown (notably the extracellular domains of all four glycophorins); we have also omitted all glycosylation from the models. However, consideration of the mass of protein and carbohydrate components missing from the extracellular regions suggests they could be easily accommodated within the models shown in Fig. 3 and Fig. 4. An interesting contrast was found on the intracellular side, where it was difficult to accommodate all the known components without extending beyond the membrane domains.

The primary information we may glean from these crude constructions are estimates for the overall dimensions of the complexes. Based on our modelling of the band 3 macro-

Table 3. Junctional complex proteins.

Protein	Copy no. ($\times 10^3$)	Oligomeric state	Size (aa)	Domain			
				Description	aa	Structure	Structure shown in figure
GPC	135 (10% free?)	Cluster?	128	Extracellular domain	1–57	Disordered (pred.)	Not shown
				Membrane domain	58–81	TM helix (pred.)	TM helix from GPA NMR structure (PDB ID: 1afo, MacKenzie et al. 1997)
				Cytoplasmic domain	82–128	Disordered (pred.)	Not shown
GPD	50	Cluster?	107	As GPC (but missing residues 1–21)	As GPC		As GPC (but missing residues 1–21)
Protein 4.1	200	Monomer	864		1–51	Disordered (pred.)	Not shown
				N-terminal domain	52–209	Highly speculative model constructed with Phyre (based on PDB ID: 2rh1, Cherezov et al. 2007)	Homology model constructed with Phyre. Very speculative.
				FERM domain	210–488	Crystal structure (PDB ID: 1gg3, Han et al. 2000)	Crystal structure. Shown in arbitrary orientation with model of N-terminal domain.
				C-terminal domain	488–864	Disordered (pred.), last 70 aa possibly folded	Not shown
p55	80	Dimer	466	N-terminal domain	1–70	Largely disordered (pred.)	Not shown
				PDZ (DHR)	69–153	NMR structures (PDB ID: 2ejy, 2ev8, Kusunoki and Kohno 2007)	NMR structure (2ejy)
				SH3 domain	158–228	SMR model for residues 161–463 (SMR accession Q00013)	SMR model. Shown in arbitary orientation with NMR structure of PDZ domain.
				Guanylate kinase-like domain	282–463		
β-Actin	500	Filament	375	Filaments of ~15–20 monomers		Atomic model (see Holmes et al. 1990)	Not shown
Dematin	140	Trimer	405	Core fragment	1–341	Largely disordered (pred.)	Not shown
				Head piece	342–405	NMR structures (PDB ID: 1zv6, Jiang and McKnight 2006)	NMR structure. Shown in an arbitary trimeric arrangement.
α-Adducin	30	Heterodimer	737	N-terminal domain	1–141	Speculative homology model constructed with Phyre (based on PDB ID: 1zym, Liao et al. 1996)	Homology model constructed with Phyre. Very speculative.
				Globular head region	142–389	SMR model, SMR accession P35611 (see also Hughes and Bennett 1995)	SMR homology model. Shown in arbitary orientation with model of N-terminal domain.
				Tail	430–737	Disordered (exp.) (Hughes and Bennett 1995)	Not shown
β-Adducin	30	Heterodimer	726	N-terminal domain	1–130	Speculative homology model constructed with Phyre (based on PDB ID: 5eau, Starks et al. 1997)	Homology model constructed with Phyre. Very speculative.
				Globular head region	131–370	SMR model, SMR accession P35612	SMR homology model. Shown in arbitary orientation with N-terminal domain.

Table 3 (*concluded*).

Protein	Copy no. ($\times 10^3$)	Oligomeric state	Size (aa)	Domain		Structure	Structure shown in figure
				Description	aa		
				Tail	409–726	Disordered (exp.) (Hughes and Bennett 1995)	Not shown
Tropomodulin	30	Monomer					Not shown
Tropomyosin	70	Dimer					Not shown
Band 3	1200 (80? in junctions)	Dimer	911	Cytoplasmic domain	1–380	Crystal structure (PDB ID: 1hyn, Zhang et al. 2000)	Crystal structure. Orientation with respect to membrane domain is highly speculative.
				Membrane domain	380–911	Low-resolution crystal structure (Yamaguchi et al. 2010)	Crystal structure of bacterial ClC Cl/H exchanger (PDB ID: 1kpl, Dutzler et al. 2002). Low-resolution AE1 crystal structure shows that bacterial ClC Cl/H exchanger shares overall size and shape with AE1 membrane domain.
Glut1	200–700	Dimer	492	MFS transporter (pred.)	1–492	Homology model available (Salas-Burgos et al. 2004)	Homology model. Expected to be of good quality.
Kell	3–18		372	Cytoplasmic domain	1–47	Disordered (pred.)	Not shown
				Membrane domain	48–67	TM helix (pred.)	Ab initio modelled ideal α-helix (MacKenzie et al. 1997)
				Extracellular, zinc endopeptidase domain	68–732	Homology model available (Karamatic Crew et al. 2010)	Homology model. Expected to be of good quality.
Kx	?		444	Membrane transport	1–444	Speculative homology model constructed with Phyre (based on PDB ID: 2cfq, Mirza et al. 2006)	Homology model constructed with Phyre. Detailed structure is very speculative.

Note: "pred.", predicted from sequence; TM, transmembrane; PDB, Protein Data Bank; "exp.", experimental data available; SMR, SWISS-MODEL Repository of homology models; Phyre, Protein Homology/analogY Recognition Engine (Kelley and Sternberg 2009).

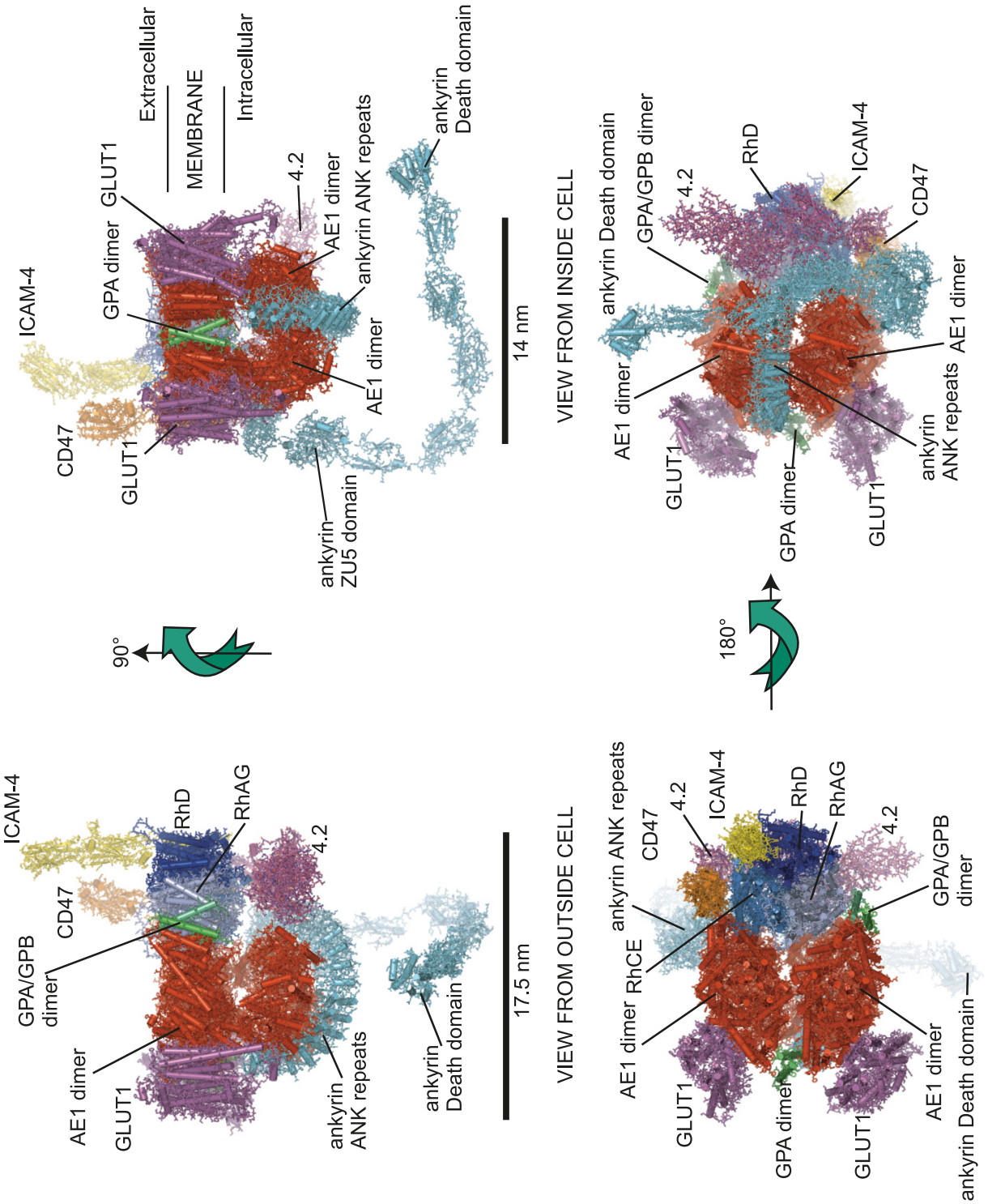

Fig. 3. Model of the band 3 macrocomplex. The components shown in the figure are as follows: two band 3 homodimers (red), one Rh–RhAG heterotrimer (RhAG light blue, RhCE medium blue, RhD dark blue), one GPA homodimer (green), one GPA–GPB heterodimer (green), one ICAM-4 monomer (yellow), one CD47 monomer (orange), one glut1 monomer (purple), one protein 4.2 monomer (magenta), and one ankyrin monomer (cyan). All components are shown with secondary structure elements highlighted as cartoons and residues also displayed in an all-atom stick representation.

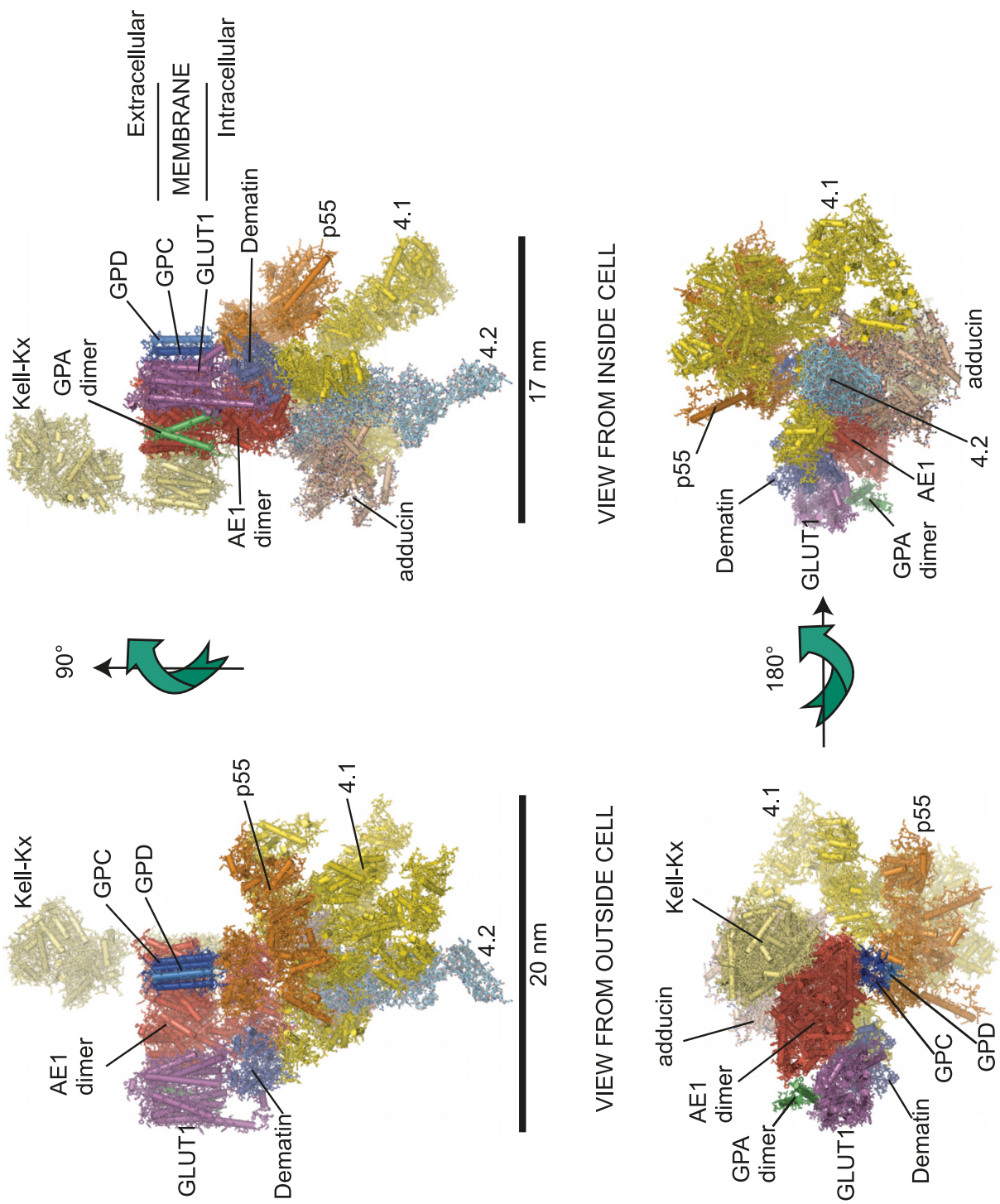

Fig. 4. Model of the protein 4.1 junctional complex. The components shown in the figure are as follows: one band 3 homodimer (red), a cluster of four GPC monomers (dark blue) and one GPD monomer (light blue), one GPA dimer (green), one glut1 monomer (purple), one Kell–Kx heterodimer (pale yellow), one protein 4.2 monomer (cyan), one dematin homotrimer (violet), one α-adducin–β-adducin heterodimer (beige), one p55 monomer (orange), and five protein 4.1 monomers (yellow). All components are shown with secondary structure elements highlighted as cartoons and residues also displayed in an all-atom stick representation.

complex, we estimate the diameter of the band 3 tetramer is ~10 nm and that of the Rh trimer is ~7.5 nm. These proteins form the core of the macrocomplex and after addition of 1.6 nm for GPA and GPB and 5 nm for glut1 (±2.5 nm for CD47), the overall size of the macrocomplex is about 245 nm^2 (17.5 nm × 14 nm as constructed in Fig. 3). Our modelling of the junctional complex suggests that the diameter of five GPC molecules is ~2 nm, that of the band 3 dimer is ~4–9 nm (depending on which axis is measured), that of glut1 is ~5 nm, and that of the GPA dimer is ~1.6 nm (±1 nm for Kell; ±4 nm for Kx). The estimated overall size for the junctional complex is about 340 nm^2 (20 nm × 17 nm as constructed in Fig. 4). Without having performed molecular modelling, one may have attempted to estimate the sizes of the complexes from a simple consideration of the number of transmembrane helices within each complex. Taking the diameter of an average α-helix to be 0.7–1.2 nm, such calculations would give areas of 62–180 nm^2 for the band 3 macrocomplex and 30–87 nm^2 for the junctional complex. These figures are considerably less than our estimates, demonstrating the importance of simulating helical packing and also considering the extent of the intracellular protein components. Indeed, as discussed above, the models were constructed to pack all the known components as tightly as possible. As the true packing may be looser, the sizes given above may still be underestimations.

It is known that a spectrin tetramer is about 200 nm long when extended (Shotton et al. 1979) but can contract to ~70 nm (Paramore et al. 2006). So when spectrin is contracted the complexes of proteins in the membrane will be crowded together. The band 3 macrocomplex will come within 2 nm of the junctional complex. Other complexes within the spectrin corrals will come in close proximity. A diagram of a single contracted corral, with the various complexes drawn to scale, is shown in Fig. 2*c*. Given that "free" band 3 dimers have lateral and rotational movement, and even complexes tethered to the cytoskeleton have some lateral movement, there is every possibility that the proteins in the different complexes can interact under certain conditions. Red cells must deform to pass through the capillaries or the splenic sinusoids (Li et al. 2007). They are also seen to "tank tread" their way through the capillaries. Yet they must maintain their biconcave disc shape to maximize their flow through the veins and arteries. Interactions between the protein complexes may signal adaptations in the membrane to achieve these deformations.

Utilizing a wealth of structural data from crystallography, NMR, and homology modelling methods, we have constructed some first, tentative models of complexes in the red cell membrane. While the details of the models are necessarily highly speculative, this approach has allowed us to generate realistic estimates of the minimum overall dimensions of the complexes. This enables us to begin extending our thoughts from the intermolecular interactions *within* these complexes to the interactions *between* them. As structural biology techniques continue to advance we will be able to replace these models with more accurate representations and continue to move along the path towards a knowledge of the true and detailed structure of the red cell membrane.

Acknowledgements

The work was supported by the Department of Health, England (L.J.B. and N.M.B.). We thank Professors David Anstee and Jean Delaunay for critical reading of this manuscript.

References

An, X., Debnath, G., Guo, X., Liu, S., Lux, S.E., Baines, A., et al. 2005. Identification and functional characterization of protein 4.1R and actin-binding sites in erythrocyte β spectrin: regulation of the interactions by phosphatidylinositol-4,5-bisphosphate. Biochemistry, **44**(31): 10681–10688. doi:10.1021/bi047331z. PMID:16060676.

An, X., and Mohandas, N. 2008. Disorders of red cell membrane. Br. J. Haematol. **141**(3): 367–375. PMID:18341630.

Anong, W.A., Franco, T., Chu, H., Weis, T.L., Devlin, E.E., Bodine, D.M., et al. 2009. Adducin forms a bridge between the erythrocyte membrane and its cytoskeleton and regulates membrane cohesion. Blood, **114**(9): 1904–1912. doi:10.1182/blood-2009-02-203216. PMID:19567882.

Anstee, D.J., Ridgwell, K., Tanner, M.J., Daniels, G.L., and Parsons, S.F. 1984. Individuals lacking the Gerbich blood-group antigen have alterations in the human erythrocyte membrane sialoglycoproteins β and γ. Biochem. J. **221**(1): 97–104. PMID: 6466322.

Anstee, D.J., and Tanner, M.J. 1988. Blood group antigen deficiencies associated with abnormal red cell shape. Blood Rev. **2**(2): 115–120. doi:10.1016/0268-960X(88)90033-1. PMID:3135867.

Anstee, D.J., Gardner, B., Spring, F.A., Holmes, C.H., Simpson, K.L., Parsons, S.F., et al. 1991. New monoclonal antibodies in CD44 and CD58: their use to quantify CD44 and CD58 on normal human erythrocytes and to compare the distribution of CD44 and CD58 in human tissues. Immunology, **74**(2): 197–205. PMID:1721039.

Becker, P.S., Schwartz, M.A., Morrow, J.S., and Lux, S.E. 1990. Radiolabel-transfer cross-linking demonstrates that protein 4.1 binds to the N-terminal region of β spectrin and to actin in binary interactions. Eur. J. Biochem. **193**(3): 827–836. doi:10.1111/j.1432-1033.1990.tb19406.x. PMID:2249696.

Bruce, L.J., Ring, S.M., Anstee, D.J., Reid, M.E., Wilkinson, S., and Tanner, M.J. 1995. Changes in the blood group Wright antigens are associated with a mutation at amino acid 658 in human erythrocyte band 3: a site of interaction between band 3 and glycophorin A under certain conditions. Blood, **85**(2): 541–547. PMID:7812009.

Bruce, L.J., Beckmann, R., Ribeiro, M.L., Peters, L.L., Chasis, J.A., Delaunay, J., et al. 2003. A band 3-based macrocomplex of integral and peripheral proteins in the RBC membrane. Blood, **101**(10): 4180–4188. doi:10.1182/blood-2002-09-2824. PMID:12531814.

Bruce, L.J. 2008. Red cell membrane transport abnormalities. Curr. Opin. Hematol. **15**(3): 184–190. doi:10.1097/MOH.0b013e3282f97b0a. PMID:18391782.

Burton, N.M., and Anstee, D.J. 2008. Structure, function and significance of Rh proteins in red cells. Curr. Opin. Hematol. **15**(6): 625–630. doi:10.1097/MOH.0b013e328311f422. PMID: 18832935.

Casey, J.R., and Reithmeier, R.A. 1991. Analysis of the oligomeric state of Band 3, the anion transport protein of the human erythrocyte membrane, by size exclusion high performance liquid chromatography. Oligomeric stability and origin of heterogeneity. J. Biol. Chem. **266**(24): 15726–15737. PMID:1874731.

Cherezov, V., Rosenbaum, D.M., Hanson, M.A., Rasmussen, S.G.,

Thian, F.S., Kobilka, T.S., et al. 2007. High-resolution crystal structure of an engineered human β_2-adrenergic G protein-coupled receptor. Science, **318**(5854): 1258–1265. doi:10.1126/science.1150577. PMID:17962520.

Daniels, G.L., Shaw, M.A., Judson, P.A., Reid, M.E., Anstee, D.J., Colpitts, P., et al. 1986. A family demonstrating inheritance of the Leach phenotype: a Gerbich-negative phenotype associated with elliptocytosis. Vox Sang. **50**(2): 117–121. doi:10.1111/j.1423-0410.1986.tb04860.x. PMID:3962280.

Daniels, G. 1995. Human blood groups. Blackwell Scientific Publications, Oxford, UK.

da Silva, P.P., and Branton, D. 1970. Membrane splitting in freeze-etching. Covalently bound ferritin as a membrane marker. J. Cell Biol. **45**(3): 598–605. doi:10.1083/jcb.45.3.598. PMID:4918216.

Delaunay, J. 2007. The molecular basis of hereditary red cell membrane disorders. Blood Rev. **21**(1): 1–20. doi:10.1016/j.blre.2006.03.005. PMID:16730867.

DeVeber, L.L., Clark, G.W., Hunking, M., and Stroup, M. 1971. Maternal anti-LW. Transfusion, **11**(1): 33–35. doi:10.1111/j.1537-2995.1971.tb04372.x. PMID:5313203.

Dutzler, R., Campbell, E.B., Cadene, M., Chait, B.T., and MacKinnon, R. 2002. X-ray structure of a ClC chloride channel at 3.0 Å reveals the molecular basis of anion selectivity. Nature, **415**(6869): 287–294. doi:10.1038/415287a. PMID:11796999.

Eyers, S.A., Ridgwell, K., Mawby, W.J., and Tanner, M.J. 1994. Topology and organization of human Rh (rhesus) blood group-related polypeptides. J. Biol. Chem. **269**(9): 6417–6423. PMID:8119991.

Fletcher, A., Bryant, J.A., Gardner, B., Judson, P.A., Spring, F.A., Parsons, S.F., et al. 1992. New monoclonal antibodies in CD59: use for the analysis of peripheral blood cells from paroxysmal nocturnal haemoglobinuria (PNH) patients and for the quantitation of CD59 on normal and decay accelerating factor (DAF)-deficient erythrocytes. Immunology, **75**(3): 507–512. PMID:1374058.

Gallagher, P.G. 2004. Hereditary elliptocytosis: spectrin and protein 4.1R. Semin. Hematol. **41**(2): 142–164. doi:10.1053/j.seminhematol.2004.01.003. PMID:15071791.

Gardner, B., Parsons, S.F., Merry, A.H., and Anstee, D.J. 1989. Epitopes on sialoglycoprotein α: evidence for heterogeneity in the molecule. Immunology, **68**(2): 283–289. PMID:2478454.

Gardner, B., Anstee, D.J., Mawby, W.J., Tanner, M.J., and von dem Borne, A.E. 1991. The abundance and organization of polypeptides associated with antigens of the Rh blood group system. Transfus. Med. **1**(2): 77–85. doi:10.1111/j.1365-3148.1991.tb00013.x. PMID:9259831.

Goodman, S.R., Yu, J., Whitfield, C.F., Culp, E.N., and Posnak, E.J. 1982. Erythrocyte membrane skeletal protein bands 4.1 a and b are sequence-related phosphoproteins. J. Biol. Chem. **257**(8): 4564–4569. PMID:7068651.

Grigorieff, N., Ceska, T.A., Downing, K.H., Baldwin, J.M., and Henderson, R. 1996. Electron-crystallographic refinement of the structure of bacteriorhodopsin. J. Mol. Biol. **259**(3): 393–421. doi:10.1006/jmbi.1996.0328. PMID:8676377.

Groves, J.D., and Tanner, M.J. 1992. Glycophorin A facilitates the expression of human band 3-mediated anion transport in *Xenopus* oocytes. J. Biol. Chem. **267**(31): 22163–22170. PMID:1385395.

Gruswitz, F., Chaudhary, S., Ho, J.D., Schlessinger, A., Pezeshki, B., Ho, C.M., et al. 2010. Function of human Rh based on structure of RhCG at 2.1 Å. Proc. Natl. Acad. Sci. U.S.A. **107**(21): 9638–9643. doi:10.1073/pnas.1003587107. PMID:20457942.

Han, B.-G., Nunomura, W., Takakuwa, Y., Mohandas, N., and Jap, B.K. 2000. Protein 4.1R core domain structure and insights into regulation of cytoskeletal organization. Nat. Struct. Biol. **7**(10): 871–875. doi:10.1038/82819. PMID:11017195.

Hatherley, D., Graham, S.C., Turner, J., Harlos, K., Stuart, D.I., and Barclay, A.N. 2008. Paired receptor specificity explained by structures of signal regulatory proteins alone and complexed with CD47. Mol. Cell, **31**(2): 266–277. doi:10.1016/j.molcel.2008.05.026. PMID:18657508.

Hemming, N.J., Anstee, D.J., Staricoff, M.A., Tanner, M.J., and Mohandas, N. 1995. Identification of the membrane attachment sites for protein 4.1 in the human erythrocyte. J. Biol. Chem. **270**(10): 5360–5366. doi:10.1074/jbc.270.10.5360. PMID:7890649.

Holmes, K.C., Popp, D., Gebhard, W., and Kabsch, W. 1990. Atomic model of the actin filament. Nature, **347**(6288): 44–49. doi:10.1038/347044a0. PMID:2395461.

Hughes, C.A., and Bennett, V. 1995. Adducin: a physical model with implications for function in assembly of spectrin–actin complexes. J. Biol. Chem. **270**(32): 18990–18996. doi:10.1074/jbc.270.32.18990. PMID:7642559.

Ipsaro, J.J., Huang, L., and Mondragón, A. 2009. Structures of the spectrin–ankyrin interaction binding domains. Blood, **113**(22): 5385–5393. doi:10.1182/blood-2008-10-184358. PMID:19141864.

Jay, D., and Cantley, L. 1986. Structural aspects of the red cell anion exchange protein. Annu. Rev. Biochem. **55**(1): 511–538. doi:10.1146/annurev.bi.55.070186.002455. PMID:3527050.

Jiang, Z.G., and McKnight, C.J. 2006. A phosphorylation-induced conformation change in dematin headpiece. Structure, **14**(2): 379–387. doi:10.1016/j.str.2005.11.007. PMID:16472756.

Karamatic Crew, V., Poole, J., Watson, T., Bullock, T., Burton, N., and Daniels, G. 2010. KASH (KEL34): A novel high incidence antigen in the Kell blood group system. Vox Sang. **99**(Suppl. 1): 357. [Abstract.]

Kato-Yamazaki, M., Okuda, H., Kawano, M., Omi, T., Iwamoto, T., Ishimori, T., et al. 2000. Molecular genetic analysis of the Japanese amorph Rh_{null} phenotype. Transfusion, **40**(5): 617–618. doi:10.1046/j.1537-2995.2000.40050617.x. PMID:10827273.

Kelley, L.A., and Sternberg, M.J.E. 2009. Protein structure prediction on the Web: a case study using the Phyre server. Nat. Protoc. **4**(3): 363–371. doi:10.1038/nprot.2009.2. PMID:19247286.

Khan, A.A., Hanada, T., Mohseni, M., Jeong, J.J., Zeng, L., Gaetani, M., et al. 2008. Dematin and adducin provide a novel link between the spectrin cytoskeleton and human erythrocyte membrane by directly interacting with glucose transporter-1. J. Biol. Chem. **283**(21): 14600–14609. doi:10.1074/jbc.M707818200. PMID:18347014.

Kiefer, F., Arnold, K., Künzli, M., Bordoli, L., and Schwede, T. 2009. The SWISS-MODEL Repository and associated resources. Nucleic Acids Res. **37**(Database issue): D387–D392. doi:10.1093/nar/gkn750. PMID:18931379.

Klein, H.G., and Anstee, D.J. 2005. Mollison's blood transfusion in clinical medicine. 11th ed. Blackwell Publishing Ltd., Oxford, UK.

Kodippili, G.C., Spector, J., Kang, G.E., Liu, H., Wickrema, A., Ritchie, K., and Low, P.S. 2010. Analysis of the kinetics of band 3 diffusion in human erythroblasts during assembly of the erythrocyte membrane skeleton. Br. J. Haematol. **150**(5): 592–600. doi:10.1111/j.1365-2141.2010.08268.x. PMID:20553270.

Korsgren, C., Peters, L.L., and Lux, S.E. 2010. Protein 4.2 binds to the carboxyl-terminal EF-hands of erythroid α-spectrin in a calcium- and calmodulin-dependent manner. J. Biol. Chem. **285**(7): 4757–4770. doi:10.1074/jbc.M109.056200. PMID:20007969.

Kusunoki, H., and Kohno, T. 2007. Structural insight into the interaction between the p55 PDZ domain and glycophorin C. Biochem. Biophys. Res. Commun. **359**(4): 972–978. doi:10.1016/j.bbrc.2007.05.215. PMID:17572384.

La-Borde, P.J., Stabach, P.R., Simonović, I., Morrow, J.S., and Simonović, M. 2010. Ankyrin recognizes both surface character and shape of the 14–15 di-repeat of β-spectrin. Biochem. Biophys. Res. Commun. **392**(4): 490–494. doi:10.1016/j.bbrc.2010.01.046. PMID:20079712.

Li, J., Lykotrafitis, G., Dao, M., and Suresh, S. 2007. Cytoskeletal dynamics of human erythrocyte. Proc. Natl. Acad. Sci. U.S.A. **104**(12): 4937–4942. doi:10.1073/pnas.0700257104. PMID:17360346.

Liao, D.I., Silverton, E., Seok, Y.J., Lee, B.R., Peterkofsky, A., and Davies, D.R. 1996. The first step in sugar transport: crystal structure of the amino terminal domain of enzyme I of the *E. coli* PEP: sugar phosphotransferase system and a model of the phosphotransfer complex with HPr. Structure, **4**(7): 861–872. doi:10.1016/S0969-2126(96)00092-5. PMID:8805571.

Liu, S.C., Derick, L.H., and Palek, J. 1987. Visualization of the hexagonal lattice in the erythrocyte membrane skeleton. J. Cell Biol. **104**(3): 527–536. doi:10.1083/jcb.104.3.527. PMID:2434513.

Liu, S.C., Palek, J., Yi, S.J., Nichols, P.E., Derick, L.H., Chiou, S.S., et al. 1995. Molecular basis of altered red blood cell membrane properties in Southeast Asian ovalocytosis: role of the mutant band 3 protein in band 3 oligomerization and retention by the membrane skeleton. Blood, **86**(1): 349–358. PMID:7795244.

Liumbruno, G., D'Alessandro, A., Grazzini, G., and Zolla, L. 2010. Blood-related proteomics. J. Proteomics, **73**(3): 483–507. doi:10.1016/j.jprot.2009.06.010. PMID:19567275.

Lux, S.E., and Palek, J. 1995. Disorders of the red cell membrane. *In* Blood: principles & practice of hematology. *Edited by* R.I. Handin, S.E. Lux, and T.P. Stossel. Lippincott Williams & Wilkins, Pa.

MacKenzie, K.R., Prestegard, J.H., and Engelman, D.M. 1997. A transmembrane helix dimer: structure and implications. Science, **276**(5309): 131–133. doi:10.1126/science.276.5309.131. PMID:9082985.

Mannuzzu, L.M., Moronne, M.M., and Macey, R.I. 1993. Estimate of the number of urea transport sites in erythrocyte ghosts using a hydrophobic mercurial. J. Membr. Biol. **133**(1): 85–97. PMID:8391582.

Marchesi, V.T., and Steers, E., Jr. 1968. Selective solubilization of a protein component of the red cell membrane. Science, **159**(3811): 203–204. doi:10.1126/science.159.3811.203. PMID:5634911.

Merry, A.H., Gardner, B., Parsons, S.F., and Anstee, D.J. 1987. Estimation of the number of binding sites for a murine monoclonal anti-Lub on human erythrocytes. Vox Sang. **53**(1): 57–60. doi:10.1111/j.1423-0410.1987.tb04915.x. PMID:3660770.

Michaely, P., and Bennett, V. 1995. The ANK repeats of erythrocyte ankyrin form two distinct but cooperative binding sites for the erythrocyte anion exchanger. J. Biol. Chem. **270**(37): 22050–22057. doi:10.1074/jbc.270.37.22050. PMID:7665627.

Michaely, P., Tomchick, D.R., Machius, M., and Anderson, R.G. 2002. Crystal structure of a 12 ANK repeat stack from human ankyrinR. EMBO J. **21**(23): 6387–6396. doi:10.1093/emboj/cdf651. PMID:12456646.

Mirza, O., Guan, L., Verner, G., Iwata, S., and Kaback, H.R. 2006. Structural evidence for induced fit and a mechanism for sugar/H^+ symport in LacY. EMBO J. **25**(6): 1177–1183. doi:10.1038/sj.emboj.7601028. PMID:16525509.

Mische, S.M., Mooseker, M.S., and Morrow, J.S. 1987. Erythrocyte adducin: a calmodulin-regulated actin-bundling protein that stimulates spectrin–actin binding. J. Cell Biol. **105**(6): 2837–2845. doi:10.1083/jcb.105.6.2837. PMID:3693401.

Nicolas, V., Le Van Kim, C., Gane, P., Birkenmeier, C., Cartron, J.P., Colin, Y., and Mouro-Chanteloup, I. 2003. Rh-RhAG/ankyrin-R, a new interaction site between the membrane bilayer and the red cell skeleton, is impaired by Rh_{null}-associated mutation. J. Biol. Chem. **278**(28): 25526–25533. doi:10.1074/jbc.M302816200. PMID:12719424.

Paramore, S., Ayton, G.S., Mirijanian, D.T., and Voth, G.A. 2006. Extending a spectrin repeat unit. I: linear force-extension response. Biophys. J. **90**(1): 92–100. doi:10.1529/biophysj.105.066969. PMID:16227506.

Parsons, S.F., Gardner, B., and Anstee, D.J. 1993. Monoclonal antibodies against Kell glycoprotein: serology, immunochemistry and quantification of antigen sites. Transfus. Med. **3**(2): 137–142. doi:10.1111/j.1365-3148.1993.tb00051.x. PMID:7690639.

Preston, G.M., Smith, B.L., Zeidel, M.L., Moulds, J.J., and Agre, P. 1994. Mutations in aquaporin-1 in phenotypically normal humans without functional CHIP water channels. Science, **265**(5178): 1585–1587. doi:10.1126/science.7521540. PMID:7521540.

Race, R.R., and Sanger, R. 1975. Blood groups in man. 6th ed. Blackwell Scientific Publications, Oxford, UK.

Reid, M.E., and Lomas-Francis, C. 2004. Blood group antigens facts book. 2nd ed. Academic Press, San Diego, Calif.

Ribeiro, M.L., Alloisio, N., Almeida, H., Gomes, C., Texier, P., Lemos, C., et al. 2000. Severe hereditary spherocytosis and distal renal tubular acidosis associated with the total absence of band 3. Blood, **96**(4): 1602–1604. PMID:10942416.

Ridgwell, K., Eyers, S.A., Mawby, W.J., Anstee, D.J., and Tanner, M.J. 1994. Studies on the glycoprotein associated with Rh (rhesus) blood group antigen expression in the human red blood cell membrane. J. Biol. Chem. **269**(9): 6410–6416. PMID:7509803.

Rinehart, J., Gulcicek, E.E., Joiner, C.H., Lifton, R.P., and Gallagher, P.G. 2010. Determinants of erythrocyte hydration. Curr. Opin. Hematol. **17**(3): 191–197. PMID:20182354.

Riwom, S., Janvier, D., Navenot, J.M., Benbunan, M., Muller, J.Y., and Blanchard, D. 1994. Production of a new murine monoclonal antibody with Fy6 specificity and characterization of the immunopurified N-glycosylated Duffy-active molecule. Vox Sang. **66**(1): 61–67. doi:10.1111/j.1423-0410.1994.tb00279.x. PMID:8146985.

Salas-Burgos, A., Iserovich, P., Zuniga, F., Vera, J.C., and Fischbarg, J. 2004. Predicting the three-dimensional structure of the human facilitative glucose transporter glut1 by a novel evolutionary homology strategy: insights on the molecular mechanism of substrate migration, and binding sites for glucose and inhibitory molecules. Biophys. J. **87**(5): 2990–2999. doi:10.1529/biophysj.104.047886. PMID:15326030.

Salomao, M., Zhang, X., Yang, Y., Lee, S., Hartwig, J.H., Chasis, J.A., et al. 2008. Protein 4.1R-dependent multiprotein complex: new insights into the structural organization of the red blood cell membrane. Proc. Natl. Acad. Sci. U.S.A. **105**(23): 8026–8031. doi:10.1073/pnas.0803225105. PMID:18524950.

Satchwell, T.J., Shoemark, D.K., Sessions, R.B., and Toye, A.M. 2009. Protein 4.2: a complex linker. Blood Cells Mol. Dis. **42**(3): 201–210. doi:10.1016/j.bcmd.2009.01.005. PMID:19269200.

Schrier, S.L. 1963. Studies of the metabolism of human erythrocyte membranes. J. Clin. Invest. **42**(6): 756–766. doi:10.1172/JCI104768. PMID:13987053.

Shotton, D.M., Burke, B.E., and Branton, D. 1979. The molecular

structure of human erythrocyte spectrin. Biophysical and electron microscopic studies. J. Mol. Biol. **131**(2): 303–329. doi:10.1016/0022-2836(79)90078-0. PMID:490648.

Smythe, J., Gardner, B., and Anstee, D.J. 1994. Quantitation of the number of molecules of glycophorins C and D on normal red blood cells using radioiodinated Fab fragments of monoclonal antibodies. Blood, **83**(6): 1668–1672. PMID:8123859.

Spring, F.A., Parsons, S.F., Ortlepp, S., Olsson, M.L., Sessions, R., Brady, R.L., and Anstee, D.J. 2001. Intercellular adhesion molecule-4 binds $\alpha_4\beta_1$ and α_V-family integrins through novel integrin-binding mechanisms. Blood, **98**(2): 458–466. doi:10.1182/blood.V98.2.458. PMID:11435317.

Stabach, P.R., Simonović, I., Ranieri, M.A., Aboodi, M.S., Steitz, T.A., Simonović, M., and Morrow, J.S. 2009. The structure of the ankyrin-binding site of β-spectrin reveals how tandem spectrin-repeats generate unique ligand-binding properties. Blood, **113**(22): 5377–5384. doi:10.1182/blood-2008-10-184291. PMID:19168783.

Starks, C.M., Back, K., Chappell, J., and Noel, J.P. 1997. Structural basis for cyclic terpene biosynthesis by tobacco 5-epi-aristolochene synthase. Science, **277**(5333): 1815–1820. doi:10.1126/science.277.5333.1815. PMID:9295271.

Steck, T.L. 1978. The band 3 protein of the human red cell membrane: A review. J. Supramol. Struct. **8**(3): 311–324. doi:10.1002/jss.400080309. PMID:364194.

Steck, T.L., Weinstein, R.S., Straus, J.H., and Wallach, D.F. 1970. Inside-out red cell membrane vesicles: preparation and purification. Science, **168**(3928): 255–257. doi:10.1126/science.168.3928.255. PMID:5418644.

Sterling, D., Reithmeier, R.A., and Casey, J.R. 2001. A transport metabolon. Functional interaction of carbonic anhydrase II and chloride/bicarbonate exchangers. J. Biol. Chem. **276**(51): 47886–47894. PMID:11606574.

Thevenin, B.J., and Low, P.S. 1990. Kinetics and regulation of the ankyrin–band 3 interaction of the human red blood cell membrane. J. Biol. Chem. **265**(27): 16166–16172. PMID:2144526.

Uversky, V.N., and Dunker, A.K. 2010. Understanding protein nonfolding. Biochim. Biophys. Acta, **1804**(6): 1231–1264. PMID:20117254.

von Castelmur, E., Marino, M., Svergun, D.I., Kreplak, L., Ucurum-Fotiadis, Z., Konarev, P.V., et al. 2008. A regular pattern of Ig super-motifs defines segmental flexibility as the elastic mechanism of the titin chain. Proc. Natl. Acad. Sci. U.S.A. **105**(4): 1186–1191. doi:10.1073/pnas.0707163105. PMID:18212128.

Weber, A., Pennise, C.R., Babcock, G.G., and Fowler, V.M. 1994. Tropomodulin caps the pointed ends of actin filaments. J. Cell Biol. **127**(6): 1627–1635. doi:10.1083/jcb.127.6.1627. PMID:7798317.

Yamaguchi, T., Ikeda, Y., Abe, Y., Kuma, H., Kang, D., Hamasaki, N., and Hirai, T. 2010. Structure of the membrane domain of human erythrocyte anion exchanger 1 revealed by electron crystallography. J. Mol. Biol. **397**(1): 179–189. doi:10.1016/j.jmb.2010.01.027. PMID:20100494.

Yawata, Y. 2003. Cell membrane: the red blood cell as a model. WILEY-VCH Verlag GmbH & Co., Weinheim, Germany. pp. 47–59.

Zhang, D., Kiyatkin, A., Bolin, J.T., and Low, P.S. 2000. Crystallographic structure and functional interpretation of the cytoplasmic domain of erythrocyte membrane band 3. Blood, **96**(9): 2925–2933. PMID:11049968.